DOI: 10.1002/chem.201001278

The Versatile Coordination Modes of Monophosphine-*o*-Carborane in the Formation of Iridium and Rhodium Complexes: Synthesis, Reactivity, and Characterization

Xian-Kuan Huo, Ge Su, and Guo-Xin Jin*[a]

Abstract: Monophosphine-*o*-carborane has four competitive coordination modes when it coordinates to metal centers. To explore the structural transitions driven by these competitive coordination modes, a series of monophosphine-*o*-carborane Ir,Rh complexes were synthesized and characterized. $[Cp^*M(Cl)_2\{1\text{-}(PPh_2)\text{-}1,2\text{-}C_2B_{10}H_{11}\}]$ (M = Ir (**1a**), Rh (**1b**); $Cp^* = \eta^5\text{-}C_5Me_5$), $[Cp^*Ir(H)\{7\text{-}(PPh_2)\text{-}7,8\text{-}C_2B_9H_{11}\}]$ (**2a**), and $[1\text{-}(PPh_2)\text{-}3\text{-}(\eta^5\text{-}Cp^*)\text{-}3,1,2\text{-}MC_2B_9H_{10}]$ (M = Ir (**3a**), Rh (**3b**)) can be all prepared directly by the reaction of $1\text{-}(PPh_2)\text{-}1,2\text{-}C_2B_{10}H_{11}$ with dimeric complexes $[(Cp^*MCl_2)_2]$ (M = Ir, Rh) under different conditions. Compound **3b** was treated with AgOTf ($OTf = CF_3SO_3^-$) to afford the tetranuclear metallacarborane $[Ag_2(thf)_2(OTf)_2\{1\text{-}(PPh_2)\text{-}3\text{-}(\eta^5\text{-}Cp^*)\text{-}3,1,2\text{-}RhC_2B_9H_{10}\}_2]$ (**4b**). The arylphosphine group in **3a** and **3b** was functionalized by elemental sulfur (1 equiv) in the presence of Et_3N to afford $[1\text{-}\{(S)PPh_2\}\text{-}3\text{-}(\eta^5\text{-}Cp^*)\text{-}3,1,2\text{-}MC_2B_9H_{10}]$ (M = Ir (**5a**), Rh (**5b**)). Additionally, the $1\text{-}(PPh_2)\text{-}1,2\text{-}C_2B_{10}H_{11}$ ligand was functionalized by elemental sulfur (2 equiv) and then treated with $[(Cp^*IrCl_2)_2]$, thus resulting in two 16-electron complexes $[Cp^*Ir(7\text{-}\{(S)PPh_2\}\text{-}8\text{-}S\text{-}7,8\text{-}C_2B_9H_9)]$ (**6a**) and $[Cp^*Ir(7\text{-}\{(S)PPh_2\}\text{-}8\text{-}S\text{-}9\text{-}OCH_3\text{-}7,8\text{-}C_2B_9H_9)]$ (**7a**). Compound **6a** further reacted with nBuPPh$_2$, thereby leading to 18-electron complex $[Cp^*Ir(n\text{BuPPh}_2)(7\text{-}\{(S)PPh_2\}\text{-}8\text{-}S\text{-}7,8\text{-}C_2B_9H_{10})]$ (**8a**). The influences of other factors on structural transitions or the formation of targeted compounds, including reaction temperature and solvent, were also explored.

Keywords: carboranes · coordination modes · iridium · rhodium · structural transitions

Introduction

In material science or chemical research, rational design of new *o*-carborane-derived materials have attracted much attention,[1] not only for their aesthetic and fascinating structures,[2] but also for their various applications in boron–neutron capture therapy,[3] catalysis,[4a–e] nuclear-waste remediation,[4f–h] and ion-selective electrodes.[4i] Undoubtedly, monophosphine-*o*-carborane is one of most attractive starting precursors[1–3,5] because it has a high tendency to coordinate to metal centers with its lone pair and it has one arylphosphine group that can satisfactorily stabilize the metal ion with bulky steric effects.[4b] Although in most cases the P atom in monophosphine-*o*-carborane prefers to coordinate to the metal center, examples have been reported that the B and C_{cage} atoms of *o*-carborane and even the pentagonal open face of *nido*-carborane degraded from *closo*-carborane can also act as coordination sites.[6] All of these coordination modes lead to abundant structural motifs. Of course, certain conditions are required to achieve the complexes that bear these respective coordination modes.[6]

To find out which factor plays the decisive role in the structural transitions, we describe here a series of half-sandwich iridium and rhodium complexes synthesized under different conditions (Scheme 1). First, $[Cp^*M(Cl)_2\{1\text{-}(PPh_2)\text{-}1,2\text{-}C_2B_{10}H_{11}\}]$ (M = Ir (**1a**), Rh (**1b**); $Cp^* = \eta^5\text{-}C_5Me_5$) was prepared by the reaction of $1\text{-}(PPh_2)\text{-}1,2\text{-}C_2B_{10}H_{11}$ with dimeric complexes $[\{Cp^*MCl_2\}_2]$ (M = Ir, Rh) by utilizing Et_3N as the weak base in tetrahydrofuran (THF). Second, $1\text{-}(PPh_2)\text{-}1,2\text{-}C_2B_{10}H_{11}$ was treated with dimeric complex $[\{Cp^*IrCl_2\}_2]$ in CH_3OH with NaOAc base under a dihydrogen atmosphere to result in metal–hydride complex $[Cp^*Ir(H)\{7\text{-}(PPh_2)\text{-}7,8\text{-}C_2B_9H_{11}\}]$ (**2a**) as well as the formation of B-H-M bonds, which are rare. Third, $[1\text{-}(PPh_2)\text{-}3\text{-}(\eta^5\text{-}Cp^*)\text{-}3,1,2\text{-}MC_2B_9H_{10}]$ (M = Ir (**3a**), Rh (**3b**)) was isolated directly from the reaction between $1\text{-}(PPh_2)\text{-}1,2\text{-}C_2B_{10}H_{11}$ with di-

[a] Dr. X.-K. Huo, G. Su, Prof. Dr. G.-X. Jin
Shanghai Key Laboratory of Molecular Catalysis and Innovative Material
Department of Chemistry, Fudan University
Shanghai 200433 (P.R. China)
Fax: (+86)-21-65643776
E-mail: gxjin@fudan.edu.cn

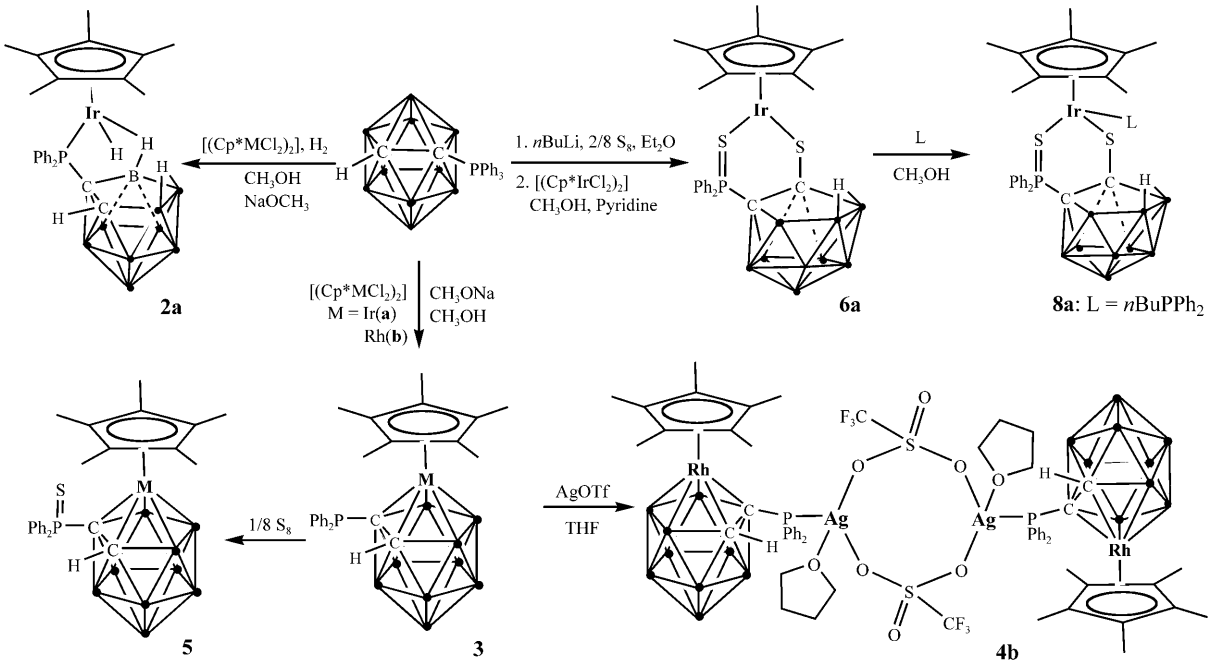

Scheme 1. Synthesis of complexes **2**–**8**.

meric complexes $[\{Cp^*MCl_2\}_2]$ (M = Ir, Rh) in CH_3OH with CH_3ONa base in high yields at room temperature; they can also be transformed from **1a** or **1b** at elevated temperature in CH_3OH in the presence of CH_3ONa. The addition of AgOTf (OTf = $CF_3SO_3^-$) to **3b** resulted in tetra-heteronuclear metallacarborane $[Ag_2(thf)_2(OTf)_2\{1\text{-}(PPh_2)\text{-}3\text{-}(\eta^5\text{-}Cp^*)\text{-}3,1,2\text{-}RhC_2B_9H_{10}\}_2]$ (**4b**). Treatments of **3a** and **3b** with elemental sulfur (1 equiv) in the presence of Et_3N afforded $[1\text{-}\{(S)PPh_2\}\text{-}3\text{-}(\eta^5\text{-}Cp^*)\text{-}3,1,2\text{-}MC_2B_9H_{10}]$ (M = Ir (**5a**), Rh (**5b**)). Additionally, the $1\text{-}(PPh_2)\text{-}1,2\text{-}C_2B_{10}H_{11}$ ligand was functionalized by elemental sulfur (2 equiv) and then treated with dimeric complex $[\{Cp^*IrCl_2\}_2]$ to afford two 16-electron complexes, $[Cp^*Ir(7\text{-}\{(S)PPh_2\}\text{-}8\text{-}S\text{-}7,8\text{-}C_2B_9H_9)]$ (**6a**) and $[Cp^*Ir(7\text{-}\{(S)PPh_2\}\text{-}8\text{-}S\text{-}9\text{-}OCH_3\text{-}7,8\text{-}C_2B_9H_9)]$ (**7a**). Compound **6a** was further treated with nBuPPh$_2$ to lead to $[Cp^*Ir(n\text{BuPPh}_2)(7\text{-}\{(S)PPh_2\}\text{-}8\text{-}S\text{-}7,8\text{-}C_2B_9H_{10})]$ (**8a**). All of these complexes were characterized by (^{1}H, ^{11}B, ^{31}P) NMR spectroscopy, IR spectroscopy, and elemental analysis, and the structures of **1a**, **2a**, **3b**, **4b**, **5a**, **5b**, **7a**, and **8a** were further confirmed by single-crystal X-ray diffraction.

Results and Discussion

Synthesis and characterization of $[Cp^*M(Cl)_2(1\text{-}PPh_2\text{-}1,2\text{-}C_2B_{10}H_{11})]$ (M = Ir (1a), Rh (1b)): Complexes $[Cp^*M(Cl)_2(1\text{-}PPh_2\text{-}1,2\text{-}C_2B_{10}H_{11})]$ (M = Ir (**1a**), Rh (**1b**)) were prepared by the reaction of dimeric complexes $[\{Cp^*MCl_2\}_2]$ (M = Ir, Rh) with $1\text{-}(PPh_2)\text{-}1,2\text{-}C_2B_{10}H_{11}$ (2 equiv; Scheme 2) in THF in the presence of Et_3N. It should be noted that the weak base is necessary for the formation of **1a** and **1b**, or the complexes cannot be isolated even at elevated temperature for 3 d. The complexes were obtained in 96% yield from recrystallization in the form of air-stable and red transparent prismatic crystals. For **1a**, the

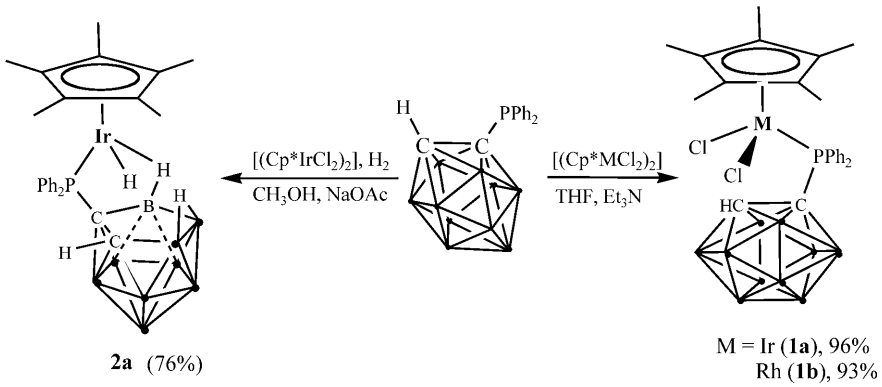

Scheme 2. Synthesis of **1a**, **1b**, and **2a**.

IR spectra show a strong band for the B–H vibration at approximately 2570 and 2554 cm^{-1}. ^1H NMR spectra show the Cp*, H–C_{cage}, and phenyl at $\delta =$ 1.07, 3.45, and 7.56–8.31 ppm, respectively. ^{11}B NMR spectra exhibit resonances at $\delta = 0.18$ (2B), −5.25 (1B), −7.34 (1B), −8.20 (2B), and −12.58 ppm (4B). ^{31}P NMR spectra exhibit a sharp signal at $\delta = 56.80$ ppm, which corresponds to M–*P*Ph_2 of the target complex. These spectroscopic data and the combustion analysis for H and C indicate the formation of a new complex [Cp*Ir$(Cl)_2$(1-PPh_2-1,2-$C_2B_{10}H_{11}$)], which was further confirmed by X-ray crystallography. For **1b**, a detailed analysis of the spectroscopic data (IR; ^1H, ^{11}B, and ^{31}P NMR spectroscopy) shows the structure is identical to **1a**, which was confirmed by elemental analysis. Suitable crystals for X-ray crystallography of **1a** were obtained by slow diffusion of hexane into concentrated solution of the complex in dichloromethane. The crystallographic data of **1a** are summarized in Table 1; an ORTEP drawing of **1a** and selected bonds and angles are shown in Figure 1. The molecular structure reveals that the geometry at the iridium(III) center is a three-legged piano-stool motif with iridium atom coordinated by the η^5-Cp*, one P atom of 1-PPh_2-1,2-$C_2B_{10}H_{11}$, and two chloride atoms; consequently, it can be described as pseudo-octahedron in which η^5-Cp* group occupies three *fac* coordination sides. The Ir–P and Ir–Cl bond lengths are comparable to those of analogous complexes.[7]

Synthesis and characterization of metal–hydride complex 2a: For borane ligands, the B–H bond can be activated by a transition metal such as Ir, Rh, or Pd, and this kind of complex has been widely used as a catalyst in organic synthesis.[7b–d] Furthermore, complexes that contain a monocoordination mode are not as stable as those that contain chelating modes.[8] Hence, we focused our attention on the synthesis of complexes that contain P,B–H chelating coordinative modes. Many efforts were devoted to the synthesis of **2a** and **2b** from staring materials 1-(PPh_2)-1,2-$C_2B_{10}H_{11}$ and [{Cp*MCl_2}$_2$] (M = Ir, Rh) or from **1a** and **1b**, but only those using **2a** were successfully isolated by the reaction from starting materials in CH_3OH in the presence of H_2 gas and NaOAc at elevated temperature (Scheme 2). Compound **2a** is soluble in a general organic solvent such as toluene, THF, CH_2Cl_2, or CH_3CN, but only partially soluble in CH_3OH. The structure of **2a** was confirmed by the detailed analysis of the spectroscopic data (IR; ^1H, ^{11}B, and ^{31}P NMR spectroscopy). The infrared spectra of **2a** show a band at 2129 cm^{-1} for Ir–H vibration; 2078 cm^{-1} for B-H-Ir; and 2581, 2563, and 2520 cm^{-1} for B–H. The ^1H NMR spectra of **2a** indicate one peak at $\delta =$

Table 1. Crystallographic data and structure refinement parameters for **1a**, **2a**, **3b**, **4b**, **5a**, **5b**, **7a**, and **8a**.

	1a	**2a**	**3b**	**4b**	**5a**	**5b**	**7a**	**8a**·CH_2Cl_2
empirical formula	$C_{24}H_{36}B_{10}Cl_2PIr$	$C_{24}H_{37}B_9IrP$	$C_{24}H_{35}B_9PRh$	$C_{58}H_{86}Ag_2B_{18}F_6O_8P_2Rh_2S_2$	$C_{24}H_{35}B_9IrPS$	$C_{24}H_{35}B_9PRhS$	$C_{25}H_{37}B_9IrOPS_2$	$C_{41}H_{56}B_9Cl_2IrP_2S_2$
formula weight	726.70	646.00	554.69	1767.47	676.04	586.75	738.13	1035.31
crystal system	orthorhombic	monoclinic	monoclinic	triclinic	monoclinic	monoclinic	monoclinic	monoclinic
space group	*Cmca*	*P*2(1)/*n*	*P*2(1)	$P\bar{1}$	*P*2(1)/*n*	*P*2(1)/*n*	*P*2(1)/*c*	*P*2(1)/*c*
a [Å]	15.000(7)	11.613(3)	9.479(3)	9.739(7)	11.573(6)	11.506(4)	15.141(10)	11.478(3)
b [Å]	25.939(12)	20.575(6)	12.540(4)	11.217(8)	18.020(9)	18.100(6)	10.075(7)	34.303(9)
c [Å]	15.467(7)	11.931(4)	11.907(4)	18.715(13)	14.318(7)	14.310(5)	21.627(15)	12.704(3)
α [°]	90	90	90	76.266(9)	90	90	90	90
β [°]	90	105.166(4)	103.800(4)	76.832(9)	113.469(6)	113.366(4)	108.749(8)	112.027(3)
γ [°]	90	90	90	70.396(8)	90	90	90	90
V [Å^3]	6018(5)	2751.4(14)	1374.4(7)	1846(2)	2739(2)	2735.8(16)	3124(4)	4637(2)
Z	8	4	2	1	–	4	4	4
ρ_{calcd} [g cm^{-3}]	1.604	1.560	1.340	1.590	1.639	1.425	1.569	1.483
μ ($Mo_{K\alpha}$) [mm^{-1}]	4.684	4.924	0.692	1.126	5.024	0.773	4.479	3.184
F(000)	2848	1272	568	888	1328	1200	1456	2080
θ range [°]	1.57–25.06	1.98–27.01	1.76–27.01	1.96–26.01	1.92–27.01	1.92–27.01	1.99–25.01	1.83–27.01
limiting indices	−17, 17	−14, 12	−10, 12	−11, 12	−9, 14	−14, 11	−17, 18	−6, 14
	−29, 30	−26, 18	−15, 16	−13, 13	−21, 22	−22, 23	−10, 11	−43, 43
	−16, 18	−15, 14	−11, 15	−22, 14	−17, 18	−17, 18	−24, 25	−16, 15
unique reflections	12092/2767	13136/5894	6577/5420	8249/6984	12918/5844	12854/5807	12227/5430	26231/9931
R(int)	0.0693	0.0349	0.0236	0.0310	0.0500	0.0398	0.0874	0.0258
completeness to θ [°]	25.06 (99.9%)	27.01 (97.9%)	27.01 (97.2%)	26.01 (96.4%)	27.01 (97.5%)	27.01 (97.0%)	25.01 (98.9%)	27.01 (98.0%)
data/restraints/params	2767/18/222	5894/1/351	5420/73/378	6984/0/460	5844/0/344	5807/0/344	5430/0/375	9931/36/572
goodness-of-fit on F^2	1.309	0.890	0.998	1.015	0.967	1.006	1.047	1.104
R_1, wR_2 [$I > 2\sigma(I)$]	0.0415, 0.1002	0.0262, 0.0489	0.0284, 0.0653	0.0344, 0.0920	0.0353, 0.0791	0.0309, 0.0765	0.0631, 0.1606	0.0297, 0.0619
*R*1, *wR*2 (all data)	0.0509, 0.1058	0.0402, 0.0510	0.0319, 0.0666	0.0402, 0.0956	0.0471, 0.0822	0.0410, 0.0808	0.1077, 0.1940	0.0365, 0.0642

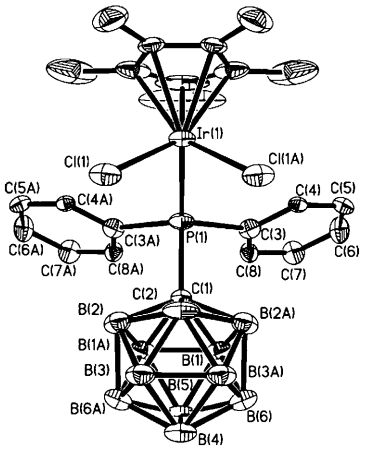

Figure 1. ORTEP drawing of **1a** with thermal ellipsoids drawn at the 30% level. All hydrogen atoms have been omitted for clarity. Selected bond lengths [Å] and angles [°]: Ir(1)–P(1) 2.321(3), Ir(1)–Cl(1) 2.393(2); P(1)-Ir(1)-Cl(1) 93.97(7), Cl(1)-Ir(1)-Cl(1A) 87.34(12).

−13.9 ppm for the Ir–H resonance; $\delta = -13.2$ ppm for the B-H-Ir resonance; and a sharp signal at $\delta = 1.83$ ppm, one signal at $\delta = 3.47$ ppm and a group of signals at $\delta = 7.40$–7.82 ppm, which can be ascribed to the Cp*, H–C_{cage}, and phenyl, respectively. ^{11}B NMR spectra exhibit resonances at $\delta = -4.97$ (1B), −8.55 (2B), −13.02 (1B), −15.61 (2B), 24.93 (1B), −27.18 (1B), and −35.13 ppm (1B). ^{31}P NMR spectra exhibit one sharp peak at $\delta = 65.58$ ppm for **2a**. To unambiguously elucidate the detailed structure, **2a** was also studied by single-crystal X-ray diffraction.

Suitable crystals for X-ray crystallography of **2a** were obtained by slow diffusion of hexane into a concentrated solution of the complex in dichloromethane. The crystallographic data of **2a** are summarized in Table 1; an ORTEP drawing of its structure and selected bonds and angles are shown in Figure 2. The molecular structure reveals that the geometry

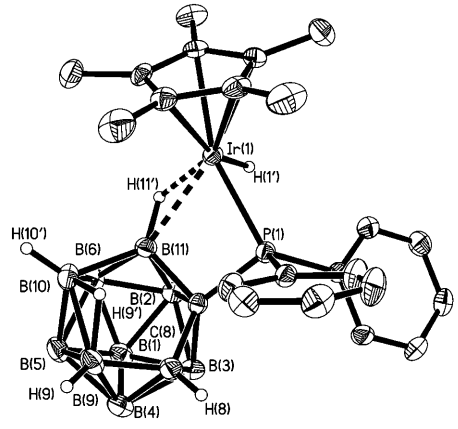

Figure 2. ORTEP drawing of **2a** with thermal ellipsoids drawn at the 30% level. All hydrogen atoms have been omitted for clarity except the hydrogen atoms on B(8), B(9), B(10), B(11), and the bridged H(9′) atom. Selected bond lengths [Å] and angles [°]: Ir(1)–P(1) 2.2727(11), Ir(1)–B(11) 2.385(4), Ir(1)–H(1′) 1.656(10), Ir(1)–H(11′) 1.71(4); P(1)-Ir(1)-H(1′) 79.0(13), B(11)-Ir(1)-H(1′) 91.5(13).

at the iridium center is a three-legged piano-stool motif, coordinated by η^5-Cp*, κ^2-[P, H-B(11)] of 7-(PPh_2)-7,8-$C_2B_9H_{11}$, and one hydrogen atom. The coordination of the [7-(PPh_2)-7,8-$C_2B_9H_{11}$]$^-$ anion to the center metal Ir atom constitutes a five-membered IrPHCB ring that is puckered at the metal center with a distance of 0.125 Å from the C(7),B(11),P(1) plane and a length of 0.660 Å between the hydrogen atom to the C(7),B(11),P(1) plane. The dihedral angles of the five-membered IrPHCB ring along the P(1) and hydrogen atoms is 161.21°. The distances of Ir–P, Ir–H(1), and Ir–H(11) are approximately 2.2727(11), 1.71(4), and 1.656(10) Å, respectively, which are all within the range of known values for them in analogous complexes.[5b,9] In addition, this complex can be regarded as a zwitterionic complex with a separated cationic metal center and the associated anionic ligand of the *nido*-carborane (Scheme 2).

Synthesis and characterization of metallacarboranes 3a and 3b: When CH_3ONa (1 equiv) was added to **1a** or **1b** in CH_3OH, and the mixture was stirred for 20 h, we found a new spot on the chromatogram when we used analytical TLC with the elution CH_2Cl_2/CH_3OH (10:1), thereby indicating the formation of a new complex. The yield of the new complex increased when the reaction was heated at reflux in CH_3OH, and the reaction was complete after 6 h (Scheme 3). When the new complexes were isolated by TLC, we found the ^{1}H NMR spectrum suffers minor changes, but the ^{11}B NMR and ^{31}P NMR spectra are completely different from **1a** or **1b**. The ^{11}B NMR spectra appear in the range of $\delta = 12$ to −28 ppm, and ^{31}P NMR spectroscopic signals appear at $\delta = 86.56$ ppm for **3a** and $\delta = 86.64$ ppm for **3b**, which are the signals of new compounds. The complexes can also be obtained in high yields from the starting materials 1-(PPh_2)-1,2-$C_2B_{10}H_{11}$ and [{Cp*MCl_2}$_2$] (M = Ir, Rh) in CH_3OH with CH_3ONa base at elevated temperature. Additionally, the structure of **3b** was confirmed by single-crystal X-ray diffraction.

Suitable crystals for X-ray crystallography of **3b** were obtained by slow diffusion of Et_2O into a concentrated solution of the complex in CH_2Cl_2. The crystallographic data of **3b** are summarized in Table 1; an ORTEP drawing of **3b** and selected bonds and angles are shown in Figure 3. From Figure 3, we can see the metal fragment Cp*Rh was further coordinated by the C_2B_3 pentagonal open face, thus resulting in the formation of a sandwich metallacarborane complex. The separation of Rh(3)–C(1) and Rh(3)–C(2) are 2.227(5) and 2.166(4) Å, respectively. This transformation can also be found in some other analogous compounds.[6]

Synthesis and characterization of metallacarborane [Ag_2-($THF)_2(OTf)_2${1-(PPh_2)-3-(η^5-Cp*)-3,1,2-$RhC_2B_9H_{10}$}$_2$] (4b): Compound **3b** and AgOTf were stirred in THF for 4 h at room temperature, thereby affording **4b** as an air-stable and red complex (Scheme 4). Compound **4b** could be purified in high yields from recrystallization as red transparent prismatic crystals. The IR spectra show a strong band for the B–H vibration at approximately 2545 and 2520 cm^{-1}, and bands

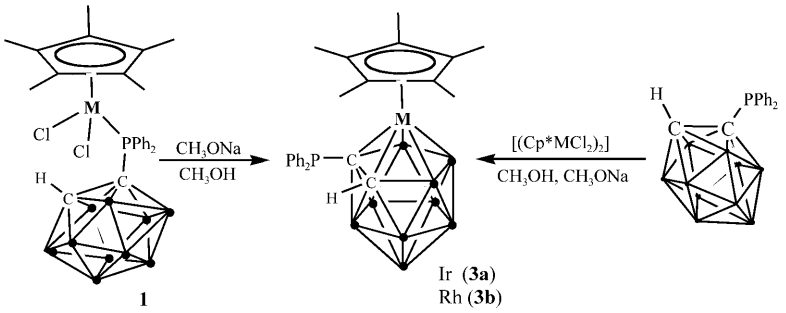

Scheme 3. Synthesis of **3a** and **3b**.

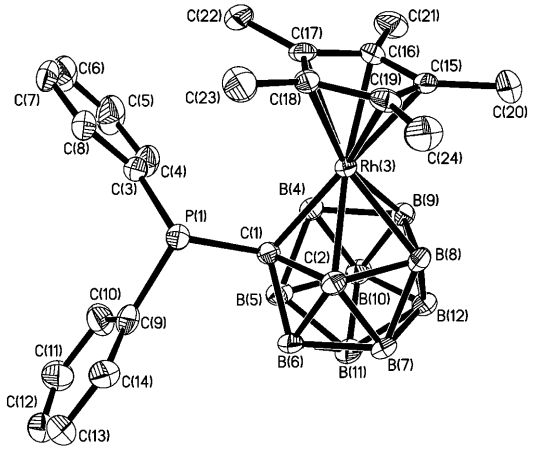

Figure 3. ORTEP drawing of **3b** with thermal ellipsoids drawn at the 30% level. All hydrogen atoms have been omitted for clarity. Selected bond lengths [Å] and angles [°]: P(1)–C(1) 1.865(5), Rh(3)–C(1) 2.227(5), Rh(3)–C(2) 2.166(4), Rh(3)–B(4) 2.160(6), Rh(3)–B(8) 2.169(3), Rh(3)–B(9) 2.190(5); P(1)-C(1)-Rh(3) 108.6(2), C(2)-C(1)-P(1) 113.2(3), B(4)-Rh(3)-C(1) 46.99(15), C(2)-Rh(3)-C(1) 45.00(18), B(8)-Rh(3)-C(1) 80.39(17), B(9)-Rh(3)-C(1) 81.13(19).

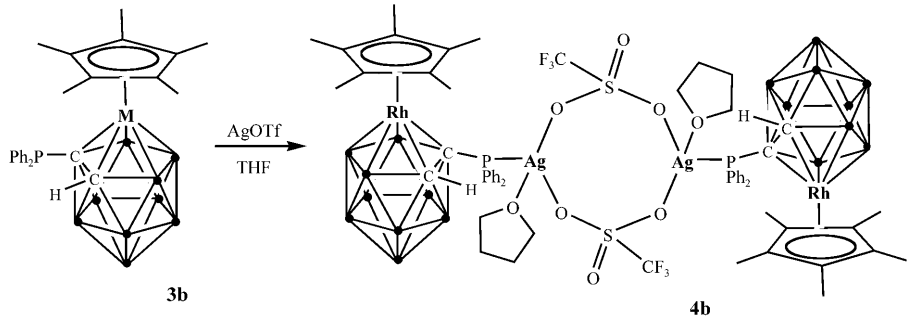

Scheme 4. Synthesis of **4b**.

for SO_3 and CF_3 vibration at approximately 1263 and 1223 cm^{-1}, respectively. The formation of **4b** is also confirmed by the appearance of a ^{31}P NMR spectroscopic signal at $\delta = 65.33$ ppm. ^{11}B NMR spectra exhibit resonances at $\delta =$ 18.17 (1B), 9.85 (1B), −2.69 (2B), −3.52 (1B), −10.32 (2B), −13.64 (1B), and −23.67 ppm (1B), which is similar to that of **3b**. The structure of **4b** was also confirmed by single-crystal X-ray diffraction.

The molecular structure of **4b** is depicted in Figure 4 and it shows that it contains one distorted eight-membered ring with its atoms symmetrically arranged at the central Ag atoms. The Ag–P bond length of 2.4125(18) Å is in the normal range for its analogous phosphorus silver complexes.[10] The Ag–O distances are 2.449(3), 2.484(4), and 2.487(3) Å in **4b**. These values compare favorably with the corresponding bond lengths in the reported Ag–O complexes.[10] The P(1)–C(1) bond length in **4b** is 1.871(3) Å, which is a little longer than that of **3b** due to its further coordination to the Ag atom. The distances of S–O are 1.432(4), 1.431(3), and 1.429(3) Å, respectively. This is different from the free OTf anion, which indicates that O(1)-S(1)-O(2) is a conjugated $^{2}_{3}\pi$ system. The bond angles around the silver atoms in the eight-membered rings are close to a right angle; the O(2)-Ag(1)-O(3) angle measures 84.05(11)°. Compound **4b** is soluble in THF, CH_2Cl_2, and CH_3OH.

Synthesis and characterization of metallacarboranes 5a and 5b: With a view toward the development of monophosphine-*o*-carborane through the formation of phosphine sulfide complexes, compounds **5a** and **5b** were synthesized and characterized. Because the oxidation usually renders the system ineffective as organometallic ligands but transforms them into flexible sulfur difunctional ligands, they may be used as ligands, extractants, photographic sensitizers, and in the manufacture of precious metals and environment protection in the near future.[11] The targeted complexes [1-P(S)Ph_2-3-(η^5-Cp*)-3,1,2-$MC_2B_9H_{10}$] (M = Ir (**5a**), Rh (**5b**)) were prepared by the reaction of **3a** or **3b** with elemental sulfur in THF heated at reflux in the presence of the weak base Et_3N (Scheme 5). The ^{31}P NMR spectra offer explicit evidence for the oxidation of the phosphorus atom ($\delta = 41.57$ ppm for **5a**; $\delta =$ 41.49 ppm for **5b**), which falls in the range expected for compounds that contain the P(S) moieties.[12] The complexes were obtained in high yields from recrystallization in the form of air-stable orange (**5a**) or red (**5b**) transparent prismatic crystals. For **5a**, ^1H NMR spectroscopic resonances appear at $\delta = 1.86$, 4.14, and 7.42–7.82 ppm, which can be ascribed to the Cp*, C_{cage}–H, and phenyl, respectively.

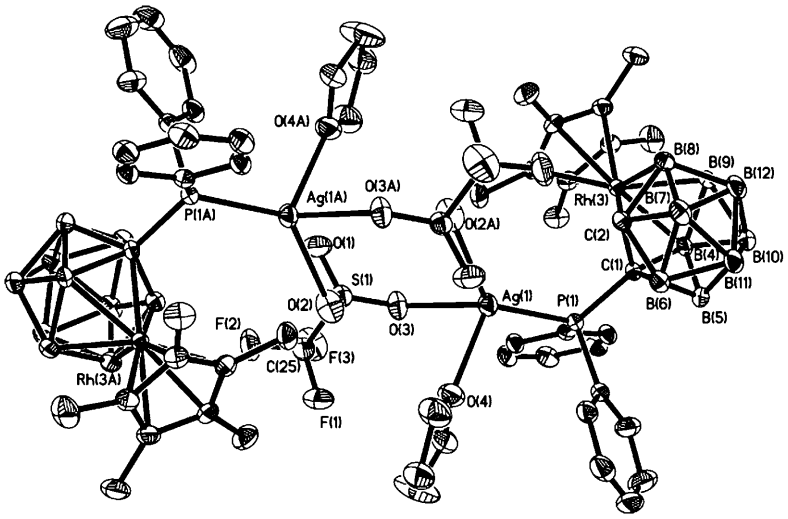

Figure 4. ORTEP drawing of **4b** with thermal ellipsoids drawn at the 30% level. All hydrogen atoms have been omitted for clarity. Selected bond lengths [Å] and angles [°]: Ag(1)–P(1) 2.4125(18), Ag(1)–O (4) 2.449(3), Ag(1)–O(2) 2.484(4), Ag(1)–O(3) 2.487(3), Rh(3)–C(1) 2.231(3), Rh(3)–C(2) 2.164(3), P(1)–C(1) 1.871(3); P(1)-Ag(1)-O(4) 109.35(8), P(1)-Ag(1)-O(2) 129.98(8), O(4)-Ag(1)-O(2) 115.31(11), P(1)-Ag(1)-O(3) 123.79(7), O(4)-Ag(1)-O(3) 82.71(12), O(2)-Ag(1)-O(3) 84.05(11), C(2)-Rh(3)-C(1) 44.84(12).

with the dimeric complex $[\{Cp^*IrCl_2\}_2]$, which will be introduced in the following text.

Synthesis and characterization of $[Cp^*Ir\{7\text{-}P(S)Ph_2\text{-}8\text{-}S\text{-}7,8\text{-}C_2B_9H_{10}\}]$ (6a) and $[Cp^*Ir\{7\text{-}P(S)Ph_2\text{-}8\text{-}S\text{-}9\text{-}OCH_3\text{-}7,8\text{-}C_2B_9H_9\}]$ (7a): Compounds **6a** and **7a** were synthesized by two steps from 1-PPh_2-1,2-$C_2B_{10}H_{11}$, *n*BuLi (1.2 equiv), elemental sulfur (2 equiv), and dimeric complex $[\{Cp^*IrCl_2\}_2]$ in the presence of pyridine at room temperature, which was purified as a green solid by column chromatography on silica gel with elution using CH_2Cl_2/CH_3OH (Scheme 6). For **6a**, the IR spectra show a strong band for the B–H vibration at approximately 2586, 2554, and 2521 cm^{-1}. ^1H NMR spectroscopic signals appear at $\delta = 1.48$ and 7.45–7.95 ppm, which can be ascribed to the Cp* and phenyl, respectively. ^{11}B NMR spectra exhibit resonances at $\delta = -2.98$ (1B), −7.56 (1B), −9.67 (1B), −15.61 (1B), −22.36 (2B), −26.99 (1B), and −33.25 ppm (2B), thus indicating the *closo*-carborane was changed into *nido*-carborane.[13] The ^{31}P NMR spectra exhibit a sharp signal at $\delta = 24.85$ ppm, which corresponds to the $-P(S)Ph_2$ group. For **7a**, the IR spectra show a strong band for the B–H vibration at approximately 2558 cm^{-1}. ^1H NMR spectroscopic signals appear at $\delta = 1.51$, 3.36, and 7.25–7.86 ppm, which can be ascribed to the Cp*,

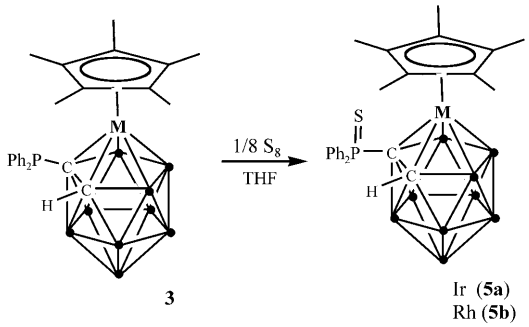

Scheme 5. Synthesis of **5a** and **5b**.

^{11}B NMR spectra exhibit resonances at $\delta = 18.17$ (1B), 9.85 (1B), −2.69 (2B), −3.52 (1B), −10.32 (2B), −13.64 (1B), and −23.67 ppm (1B). It is worth mentioning that a weak base and elevated temperature are required for the formation of **5a** and **5b**. To unambiguously confirm the presence of the P=S bond, an X-ray crystal-structure determination was performed on single crystals of **5a** and **5b** that were recrystallized from the saturated toluene solution at −18°C. As shown in Figure 5 and Figure 6, the phosphorus atom was oxidized by sulfur, thereby forming the flexible sulfur difunctional ligands. The P=S bond measures 1.952(2) Å, which is within the range of reported compounds that contain the P(S) moiety.[12] For **5b**, the bond lengths of Rh–B, Rh–C(1), and M–C(2) are all comparable to those of **3b**. To explore the reactivity of these two complexes, we utilized them as starting materials to synthesize iridium and rhodium complexes coordinated by the difunctional P,S atoms, and unfortunately the targeted complexes have not yet been successfully isolated. But we have successfully synthesized complexes **6a** and **7a** by the reaction of 1-$P(S)Ph_2$-2-S-$C_2B_{10}H_{10}$

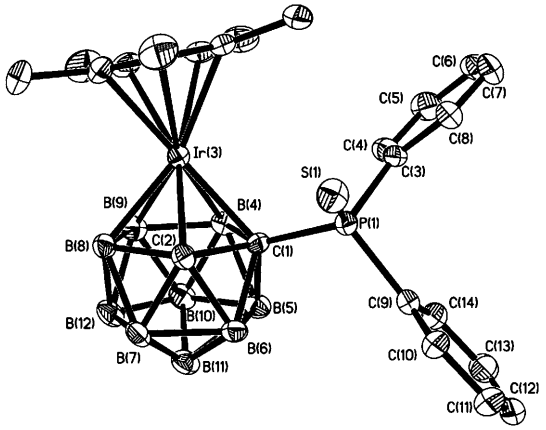

Figure 5. ORTEP drawing of **5a** with thermal ellipsoids drawn at the 30% level. All hydrogen atoms have been omitted for clarity. Selected bond lengths [Å] and angles [°]: P(1)–C(1) 1.871(5), P(1)–S(1) 1.952(2), Ir(3)–C(1) 2.214(5), Ir(3)–C(2) 2.166(5), Ir(3)–B(8) 2.180(6), Ir(3)–B(4) 2.188(5), Ir(3)–B(9) 2.213(6); C(1)-P(1)-S(1) 110.73(15), C(2)-C(1)-Ir(3) 65.6(2), P(1)-C(1)-Ir(3) 116.4(2), C(2)-Ir(3)-C(1) 45.83(17).

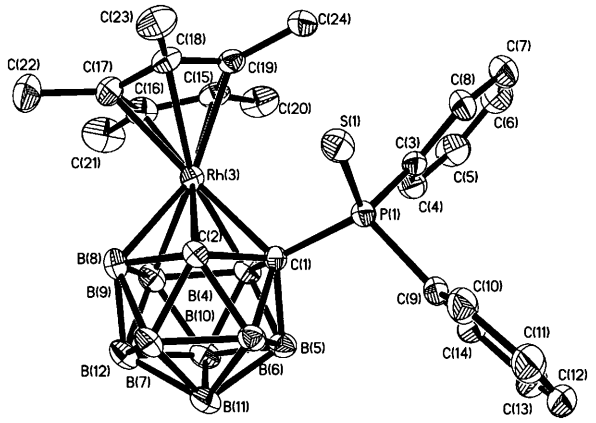

Figure 6. ORTEP drawing of **5b** with thermal ellipsoids drawn at the 30% level. All hydrogen atoms have been omitted for clarity. Selected bond lengths [Å] and angles [°]: Rh(3)–C(1) 2.230(2), Rh(3)–C(2) 2.177(2), Rh(3)–B(4) 2.186(3), Rh(3)–B(8) 2.181(3), Rh(3)–B(9) 2.203(3), P(1)–C(1) 1.875(2), P(1)–S(1) 1.9509(12); C(1)-P(1)-S(1) 110.61(8), P(1)-C(1)-Rh(3) 114.91(11), C(2)-Rh(3)-C(1) 44.25(8), B(8)-Rh(3)-C(1) 79.41(10), B(4)-Rh(3)-C(1) 47.25(9), B(9)-Rh(3)-C(1) 80.68(10).

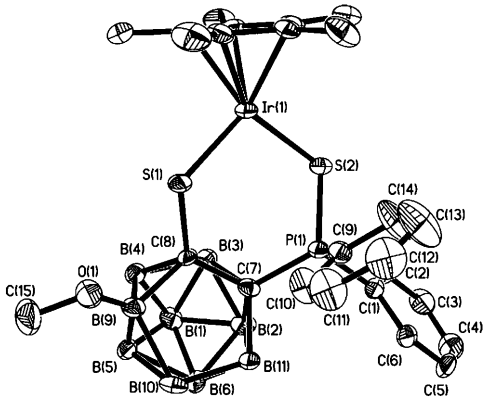

Figure 7. ORTEP drawing of **7a** with thermal ellipsoids drawn at the 30% level. All hydrogen atoms have been omitted for clarity. Selected bond lengths [Å] and angles [°]: Ir(1)–S(1) 2.229(4), Ir(1)–S(2) 2.320(4), S(1)–C(8) 1.801(11), P(1)–S(2) 2.015(5), P(1)–C(7) 1.791(13), C(7)–C(8) 1.574(19); S(1)-Ir(1)-S(2) 101.56(12), C(7)-P(1)-S(2) 115.2(5), C(8)-S(1)-Ir(1) 120.3(5).

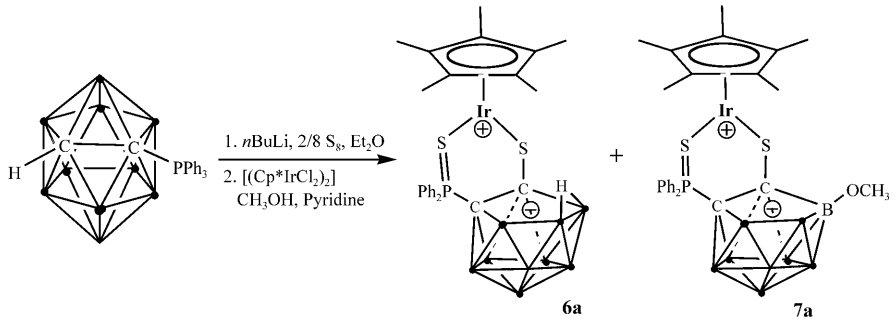

Scheme 6. Synthesis of **6a** and **7a**. The bridged H atom of **7a** between B(10) and B(11) has been omitted for clarity.

$-OCH_3$, and the phenyl, respectively. ^{11}B NMR spectra exhibit resonances at $\delta = 18.06$ (1B), -2.79 (1B), -7.81 (1B), -9.75 (1B), -11.65 (2B), -18.74 (1B), -21.97 (1B), and -33.12 ppm (1B), which suggests that the complex is also coordinated by the *nido*-carborane. The ^{31}P NMR spectra exhibit a sharp signal at $\delta = 24.76$ ppm, which corresponds to the $-P(S)Ph_2$ group. From the comparison of these spectroscopic data, the only difference between **6a** and **7a** is that **7a** has one more $-OCH_3$ substituent in the *nido*-carborane ligand. To unambiguously elucidate the detailed cluster structures of compounds **6a** and **7a**, many efforts were devoted to isolate their single crystals, but only **7a** was successfully obtained by slow diffusion of Et_2O into a concentrated solution of the complex in CH_3OH.

The crystallographic data of **7a** are summarized in Table 1. An ORTEP drawing of **7a** and selected bonds and angles are shown in Figure 7. The molecular structure reveals that the geometry at the iridium(III) is unsaturated, five-coordinated by two sulfur atoms from the 7-$P(S)Ph_2$-8-S-9-OCH_3-7,8-$C_2B_9H_9$ ligand and one Cp* ligand functionalized as a three-coordinated ligand, thereby forming a two-legged piano-stool geometry. The distorted six-membered ring is formed by the Ir(1), S(1), C(7), C(8), P(1), and S(2) atoms, with a dihedral angle of 29.57° between the Ir(1),S(1),S(2) plane and the S(1),C(7),C(8),P(1) plane. The separation between the S(2) or center Ir atom with the S(1),C(7),C(8),P(1) plane is 1.450, 1.087 Å. The dihedral angle between the Cp* plane and the S(1),C(7),C(8),P(1) plane is 75.90°, whereas the dihedral angle between the Cp* plane and the Ir(1),S(1),S(2) plane is 88.64°, which is close to a right angle. Compared with analogous complexes,[11,14] the Ir(1)–S(2) bond length (2.320(4) Å) is normal but the Ir(1)–S(1) bond length (2.229(4) Å) is much shorter than that in analogous complex **1a** (2.35 Å) and even a little shorter than that of pseudoaromatic [Cp*$IrS_2(C_2B_{10}H_{10})$] in which it is 2.257 Å.[15] The reason can be explained by π-type interactions; to alleviate coordinative unsaturation around the Ir atom, electron donation from the pπ orbital on the sulfur atom occurs to stabilize the unsaturated Ir center.[15,16] Therefore **7a** may be a good precursor for other addition reactions because of its coordinative unsaturation. Compared with the starting material monophosphino *closo*-carborane, there are two phenomena that occur in the carborane cage in **7a**: 1) one boron atom, B(3), has been removed from the mother cage, which has made the *closo*-carborane into a *nido*-carborane anion and enabled the anionic charge to be delocalized onto the pendant-ring plane

(C_2B_3); 2) the hydrogen atom on B(9) has been substituted by a methoxyl group. So this complex can be regarded as a zwitterionic complex through the separation between the cationic metal fragment (Cp*Ir) and the *nido*-carborane ligand.

From the structural analysis of **7a**, it is easy to speculate that the structure of **6a** is [Cp*Ir{7-P(S)Ph_2-8-S-7,8-$C_2B_9H_{10}$}], which was also confirmed by its further reaction with *n*BuPPh_2.

Synthesis and characterization of [Cp*Ir(*n*BuPPh_2){7-P(S)Ph_2-8-S-$C_2B_9H_{10}$}] (8a): To firmly elucidate the structure of **6a** and explore its reactivity, we investigated its reaction with *n*BuPPh_2 at elevated temperature in CH_3OH (Scheme 7). Also, **8a** was isolated as an air- and moisture-

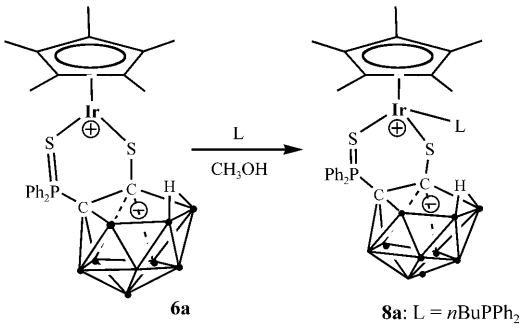

6a **8a**: L = *n*BuPPh_2

Scheme 7. Synthesis of **8a**.

stable complex after recrystallization, soluble in common organic solvents such as THF, CH_2Cl_2, toluene, and CH_3CN. The ^{31}P NMR spectra exhibit two signals for $-P(S)Ph_2$ and $-P(n\text{Bu})Ph_2$ at $\delta = 25.09$ and -3.06 ppm, respectively. The ^1H NMR spectra exhibit a group of peaks for the phenyl group at $\delta = 7.44$–7.93 ppm, and double peaks at $\delta = 1.37$ ppm with $^4J(P,H) = 2.6$ Hz for Cp*. The $-n$Bu appears at $\delta = 0.81$, 0.89, 1.67, and 1.93 ppm. These (^1H,^{31}P, ^{11}B) NMR spectroscopic data and the elemental analyses for H and C indicate that the iridium(III) center is further coordinated by the *n*BuPPh_2 ligand, which was further confirmed by X-ray crystallography.

The crystallographic data of **8a** are summarized in Table 1. An ORTEP drawing of **8a** and selected bonds and angles are shown in Figure 8. The molecular structure shows that **8a** is an 18-electron complex, and further coordinated by the *n*BuPPh_2 ligand on the basis of **6a**. The geometry of the iridium(III) center is transformed into a three-legged piano-stool shape. The Ir(1)–S(2) bond length (2.3872(10) Å) is a little longer than that of **7a**, whereas the Ir(1)–S(1) bond length (2.3872(10) Å) is much longer than that of **7a** (2.229(4) Å); all of them are comparable to those of the reported iridium complexes that contain S,S ligands.[17] The Ir(1)–S(1) bond length in **8a** becomes normal, and the reason for that may be that **8a** is an 18-electron saturated complex and the π-type interactions between the metal center and the pπ orbital on the sulfur atom in **6a**

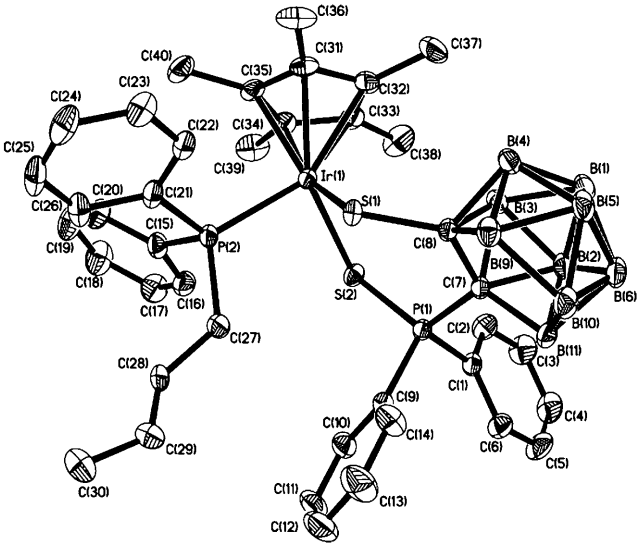

Figure 8. ORTEP drawing of **8a** with thermal ellipsoids drawn at the 30% level. All hydrogen atoms have been omitted for clarity. Selected bond lengths [Å] and angles [°]: Ir(1)–P(2) 2.3066(10), Ir(1)–S(1) 2.3872(10), Ir(1)–S(2) 2.3872(10), P(1)–S(2) 2.0367(12), C(7)–C(8) 1.578(4); P(2)-Ir(1)-S(1) 86.22(3), P(2)-Ir(1)-S(2) 92.26(3), S(1)-Ir(1)-S(2) 90.31(3), C(7)-P(1)-S(2) 119.30(11), C(8)-S(1)-Ir(1) 115.74(11).

have disappeared. It is a great coincidence that the separation of Ir(1)–S(1) is equal to that of Ir(1)–S(2) (2.3872(10) Å).

The 2.3066(10) Å distance for the Ir(1)–P(2) bond and the P=S bond length in **8a** are excellent agreement with the analogous lengths reported for other iridium complexes.[10] The angle between the Ir(1)–P(2) bond and the Ir(1),S(1),P(1) plane is 85.601°. The Cp* ring underwent a tilt of about 30.05° relative to the Ir(1),S(1),P(1) plane when **6a** was converted to **8a**. For the six-membered ring, the Ir(1),S(1),P(1) plane also underwent a tilt of about 22.02° relative to the S(1),P(1),C(7),C(8) plane when **6a** was transformed into **8a**.

Conclusion

A series of monophosphine-*o*-carborane Ir,Rh complexes were synthesized and structurally characterized. The four competitive coordination modes have led to structural transitions from the *exo*-carborane complexes (**1a**, **1b**) to carborane hydride complex **2a** or to metallacarborane compounds **3a** and **3b**. The influences of other factors on structural transitions or on the formation of target compounds, including different bases, reaction temperature, and solvent were also explored. The bimetallacarborane bridged by a Ag cation through coordination with the phosphino group of carborane (**4b**) was also isolated. Compounds **5a** and **5b** are obtained from the oxidation of **3a** and **3b** by reaction with elemental sulfur. Utilizing **5a** or **5b** with the dimeric complexes did not afford the desired complexes but we have successfully synthesized the bifunctional (P=S, S) complexes

6a and **7a**, and the reason for the stability and the reactivity of 16-electron **6a** were also preliminarily investigated.

Experimental Section

General data: All manipulations were carried out under a nitrogen atmosphere using standard Schlenk techniques unless otherwise stated. Solvents were distilled under nitrogen from sodium benzophenone (hexane, diethyl ether, THF, toluene) or calcium hydride (dichloromethane) and methanol was distilled over Mg/I_2. The starting materials 1-(PPh_2)-1,2-$C_2B_{10}H_{11}$[5c], *n*$BuPPh_2$,[18] and [{Cp*MCl_2}$_2$] (M = Ir, Rh)[19] were synthesized according to the literature. Other chemical reagents were obtained from commercial sources and used without further purification. ^{1}H (400 MHz) and ^{31}P (162 MHz) NMR spectra were measured using a VAVCE DMX-400 spectrometer. ^{11}B NMR spectra (160 MHz) were recorded using a Bruker DMX-500 spectrometer. Elemental analysis was performed using an Elementar Vario EL III analyzer. IR (KBr) spectra were measured using a Nicolet FTIR spectrophotometer.

Synthesis of 1a: [{Cp*$IrCl_2$}$_2$] (197 mg, 0.25 mmol) was added to a solution of 1-(PPh_2)-1,2-$C_2B_{10}H_{11}$ (164.2 mg, 0.5 mmol) in THF (15 mL) at 0 °C. Then Et_3N (50.5 mg, 0.5 mmol) was added to the reaction mixture after stirring for 0.5 h at 0 °C, and the mixture was stirred for 48 h at room temperature. After removal of the solvent under vacuum, **1a** was isolated by column chromatography on silica gel with elution (CH_2Cl_2/CH_3OH, 20:1). Yield: 348.8 mg (96 %) as a red solid. ^{1}H NMR(400 MHz, $CDCl_3$, 25 °C): δ = 1.07 (d, ^4J(P,H) = 2.0 Hz, 15 H; Cp*) 3.45 (s, 1 H; C_{cage}–H), 7.56–8.31 ppm (m, 10 H; phenyl); ^{11}B NMR (160 MHz, $CDCl_3$, 25 °C): δ = 0.18 (2 B), −5.25 (1 B), −7.34 (1 B), −8.20 (2 B), −12.58 ppm (4 B); ^{31}P NMR (162 MHz, $CDCl_3$, H_3PO_4, 25 °C): δ = 56.80 ppm (s; −*P*Ph_2); IR (KBr disk): $\tilde{\nu}$ = 2570, 2554 (B–H), 1381 cm^{-1} (C–H); elemental analysis calcd (%) for $C_{24}H_{36}B_{10}Cl_2PIr$: C 39.66, H 4.99; found: C 39.61, H 5.04.

Synthesis of 1b: A procedure analogous to the preparation of **1a** was used. [{Cp*$RhCl_2$}$_2$] (154.5 mg, 0.25 mmol) was added to a solution of 1-(PPh_2)-1,2-$C_2B_{10}H_{11}$ (164.2 mg, 0.5 mmol) in THF (15 mL) at 0 °C. Then Et_3N (50.5 mg, 0.5 mmol) was added to the reaction mixture after stirring for 0.5 h, and the mixture was stirred for 24 h at room temperature. Compound **1b** was isolated through recrystallization. Yield: 294.4 mg (93 %) as a dark red solid. ^{1}H NMR (400 MHz, $CDCl_3$, 25 °C): δ = 1.07 (d^4, J(P,H) = 4.2 Hz, 15 H; Cp*), 3.46 (s, 1 H; C_{cage}–H), 7.56–8.33 ppm (m, 10 H; phenyl); ^{11}B NMR (160 MHz, $CDCl_3$, 25 °C): δ = −2.52 (1 B), −4.46 (2 B), −7.13 (3 B), −9.05 (1 B), −11.38 ppm (3 B); ^{31}P NMR (162 MHz, $CDCl_3$, H_3PO_4, 25 °C): δ = 57.58 ppm (d, J(Rh,P) = 114 Hz; −*P*Ph_2); IR (KBr disk): $\tilde{\nu}$ = 2563 (B–H), 1383 cm^{-1} (C–H); elemental analysis calcd (%) for $C_{24}H_{36}B_{10}Cl_2PRh$: C 45.22, H 5.69; found: C 45.27, H 5.75.

Synthesis of 2a [{Cp*$IrCl_2$}$_2$] (197 mg, 0.25 mmol) was added to a solution of 1-(PPh_2)-1,2-$C_2B_{10}H_{11}$ (164.2 mg, 0.5 mmol) in CH_3OH (10 mL) at 0 °C. NaOAc (112.9 mg, 1 mmol) was added to the reaction mixture after stirring for 0.5 h at 0 °C, and the mixture was stirred for 24 h at room temperature in an atmosphere of dihydrogen. The mixture gradually turned yellow, coupled with some white precipitate, thereby suggesting the formation of Cp*Ir(H)(7-(PPh_2)-7,8-$C_2B_9H_{11}$) (**2a**). The solution was filtered and the solvent was removed under vacuum. Fine yellow crystals of **2a** were obtained through recrystallization from CH_2Cl_2/hexane at −18 °C. Yield: 246.1 mg (76.2 %). ^{1}H NMR (400 MHz, $CDCl_3$, 25 °C): δ = −13.99 (s, 1 H; Ir–H), −13.26 (Ir-H-B), 1.83 (d, ^4J(PH) = 4.2 Hz, 15 H; Cp*), 3.47 (s, 1 H; C_{cage}–H), 7.40–7.82 ppm (m, 10 H; phenyl); ^{11}B NMR (160 MHz, $CDCl_3$, 25 °C): δ = −4.97 (1 B), −8.55 (2 B), −13.02 (1 B), −15.61 (2 B), −24.93 (1 B), −27.18 (1 B), −35.13 ppm (1 B); ^{31}P NMR (162 MHz, $CDCl_3$, H_3PO_4, 25 °C): δ = 65.58 ppm (d, ^2J(H,P) = 12.6 Hz; −*P*Ph_2); IR (KBr disk): $\tilde{\nu}$ = 2581, 2563, 2520 (B–H), 2129 (Ir–H), 2078 (B-H-Ir), 1383 cm^{-1} (C–H); elemental analysis calcd (%) for $C_{24}H_{37}B_9IrP$: C 44.62, H 5.77; found: C 44.56, H 5.83.

Synthesis of 3a, method 1: CH_3ONa (54.0 mg, 1 mmol) was added to a solution of 1-(PPh_2)-1,2-$C_2B_{10}H_{11}$ (164.2 mg, 0.5 mmol) in CH_3OH (10 mL) at 0 °C. Then [{Cp*$IrCl_2$}$_2$] (197 mg, 0.25 mmol) was added to the reaction mixture after stirring for 0.5 h, and the mixture was heated at reflux for 24 h. The solution was filtered and the solvent was removed under vacuum. Target product **3a** was isolated by column chromatography on silica gel with elution (CH_2Cl_2/CH_3OH, 8:1). Yield: 289.8 mg (90 %) as a yellow solid. ^{1}H NMR (400 MHz, $CDCl_3$, 25 °C): δ = 1.41 (d, ^4J(P,H) = 6.2 Hz, 15 H; Cp*), 4.06 (s, 1 H; C_{cage}–H), 7.43–7.72 ppm (m, 10 H; phenyl); ^{11}B NMR (160 MHz, $CDCl_3$, 25 °C): δ = 11.07 (1 B), 9.56 (1 B), 1.21 (1 B), 0.98 (1 B), −6.75 (2 B), −15.94 (1 B), −21.84 (1 B), −27.06 ppm (1 B); ^{31}P NMR (162 MHz, $CDCl_3$, H_3PO_4, 25 °C): δ = 86.56 ppm (s; −*P*Ph_2); IR (KBr disk): $\tilde{\nu}$ = 2588, 2546 (B–H), 1383 cm^{-1} (C–H); elemental analysis calcd (%) for $C_{24}H_{35}B_9PIr$: C 44.76, H 5.48; found: C 44.71, H 5.54.

Synthesis of 3a, method 2: CH_3ONa (16.2 mg, 0.3 mmol) was added to a solution of **1a** (72.7 mg, 0.1 mmol) in CH_3OH. Then the reaction mixture was heated at reflux for 4 h. A yellow precipitate was formed when the reaction ceased. The solvent was removed under vacuum and target product **3a** was isolated by column chromatography on silica gel with elution (CH_2Cl_2/CH_3OH, 8:1). It had identical NMR spectra to the sample prepared by using method 1. Yield: 55.4 mg (86 %).

Synthesis of 3b, method 1: A procedure analogous to the preparation of **3a** was used in method 1. [{Cp*$RhCl_2$}$_2$] (154.5 mg, 0.25 mmol) was added to a mixture of 1-(PPh_2)-1,2-$C_2B_{10}H_{11}$ (164.2 mg, 0.5 mmol) and CH_3ONa (54.0 mg, 1 mmol) in CH_3OH (10 mL) at 0 °C. Then the reaction mixture was heated at reflux for 24 h, and the solvent was removed under vacuum after the solution was filtered. Target product **3b** was isolated by column chromatography on silica gel with elution (CH_2Cl_2/CH_3OH, 10:1). Yield: 241.3 mg (87 %) as a red solid. ^{1}H NMR (400 MHz, $CDCl_3$, 25 °C): δ = 1.46 (d, ^4J(P,H) = 6.4 Hz 15 H; Cp*), 4.23 (s, 1 H; C_{cage}–H), 7.28–8.12 ppm (m, 10 H; phenyl); ^{11}B NMR (160 MHz, $CDCl_3$, 25 °C): δ = 10.77 (1 B), 9.80 (1 B), 1.11 (1 B), −3.86 (1 B), −5.65 (1 B), −8.63 (2 B), −17.42 (1 B), −27.78 ppm (1 B); ^{31}P NMR (162 MHz, $CDCl_3$, H_3PO_4, 25 °C): δ = 86.64 ppm (s; −*P*Ph_2); IR (KBr disk): $\tilde{\nu}$ = 2550 (B–H), 1383 cm^{-1} (C–H); elemental analysis calcd (%) for $C_{24}H_{35}B_9PRh$: C 51.97, H 6.36; found: C 51.88, H 6.33.

Synthesis of 3b, method 2: A procedure analogous to the preparation of **3a** was used in the second method, but starting instead from **1b** (63.7 mg, 0.1 mmol) in CH_3OH. The red solid was purified by column chromatography on silica gel. It also had identical NMR spectra to the sample prepared under method 1. Yield: 50.5 mg (91 %).

Synthesis of 4b: AgOTf (25.7, 0.1 mmol) was added to a solution of **3b** (55.4 mg, 0.1 mmol) in THF (10 mL), and the mixture was stirred for 8 h. The color turned yellow from the original dark red and some gray precipitate was formed. The solvent was removed under vacuum after the solution was filtered. Compound **4b** was obtained by recrystallization from THF/hexane with a yield of 56.8 mg (64.3 %) as a yellow solid. ^{1}H NMR (400 MHz, $CDCl_3$, 25 °C): δ = 1.51 (d, ^4J(P,H) = 4.2 Hz, 30 H; Cp*), 1.87 (m, 8 H; CH_2) 4.26 (s, 2 H; C_{cage}–H), 3.75 (t, 8 H; CH_2), 7.35–7.78 ppm (m, 20 H; phenyl); ^{11}B NMR (160 MHz, $CDCl_3$, 25 °C): δ = 18.17 (1 B), 9.85 (1 B), −2.69 (2 B), −3.52 (1 B), −10.32 (2 B), −13.64 (1 B), −23.67 ppm (1 B); ^{31}P NMR (162 MHz, $CDCl_3$, H_3PO_4, 25 °C): δ = 65.33 ppm (s; −*P*Ph_2); IR (KBr disk): $\tilde{\nu}$ = 2545, 2520 (B–H), 1379 (C–H), 1263 (SO_3), 1223 cm^{-1} (CF_3); elemental analysis calcd (%) for $C_{58}H_{86}Ag_2B_{18}F_6O_8P_2Rh_2S_2$: C 39.41, H 4.90; found: C 39.53, H 4.84.

Syntheses of 5a and 5b: Element S_8 (4.8 mg, 0.015 mmol,1/8 equiv) and Et_3N (10.1 mg, 0.1 mmol, 1 equiv) were added to a solution of **3a** (64.4 mg, 0.1 mmol) or **3b** (55.4 mg, 0.1 mmol) in THF (10 mL). The solution was filtered after the mixture was heated at reflux for 24 h. The solvent was then removed under vacuum. The target complexes were obtained in yields of 48.0 mg (71 %) for **5a** and 48.7 mg (83 %) for **5b**. Fine crystals of **5a** (orange) and **5b** (red) were obtained through recrystallization from CH_2Cl_2/hexane at −18 °C.

For compound ***5a***: ^{1}H NMR (400 MHz, $CDCl_3$, 25 °C): δ = 1.86 (s, 15 H; Cp*), 4.14 (s, 1 H; C_{cage}–H), 7.42–7.82 ppm (m, 10 H; phenyl); ^{11}B NMR (160 MHz, $CDCl_3$, 25 °C): δ = 15.72 (1 B), 4.86 (1 B), −3.33 (2 B), −8.21 (2 B), −13.51 (1 B), −20.22 ppm (2 B); ^{31}P NMR (162 MHz, $CDCl_3$, H_3PO_4, 25 °C): δ = 41.57 ppm (s; −*P*(S)Ph_2); IR (KBr disk): $\tilde{\nu}$ = 2557 (B–H), 1380 (C–H), 645 cm^{-1} (P=S); elemental analysis calcd (%) for $C_{24}H_{35}B_9IrPS$: C 42.63, H 5.22; found: C 42.71, H 5.28.

For compound ***5b***: ^{1}H NMR (400 MHz, $CDCl_3$, 25 °C): $\delta = 1.86$ (s, 15H; Cp*), 4.12 (s, 1H; C_{cage}–H), 7.37–7.72 ppm (m, 10H; phenyl); ^{11}B NMR (160 MHz, $CDCl_3$, 25 °C): $\delta = 18.22$ (1B), 2.39 (1B), −3.96 (1B), −5.65 (2B), −10.73 (2B), −17.42 (1B), −27.78 ppm (1B); ^{31}P NMR (162 MHz, $CDCl_3$, H_3PO_4, 25 °C): $\delta = 41.49$ ppm (s; $-P(S)Ph_2$); IR (KBr disk): $\tilde{\nu} =$ 2550 (B–H), 1383 (C–H), 644 cm^{-1} (P=S); elemental analysis calcd (%) for $C_{24}H_{35}B_9RhPS$: C 49.12, H 6.01; found: C 49.10, H 5.96.

Syntheses of 6a and 7a: *n*BuLi in hexane (1.6 m, 0.38 mL, 0.6 mmol) was added to a solution of 1-(PPh_2)-1,2-$C_2B_{10}H_{10}$ (164 mg, 0.5 mmol) in Et_2O (15 mL) at −10 °C, and the reaction mixture was stirred for 1 h at this temperature. Then the reaction mixture was stirred overnight at room temperature. Elemental sulfur (32.0 mg, 1 mmol, 2 equiv) was added at −10 °C, and the reaction mixture was heated at reflux for a further 6 h to obtain a light yellow solution. The Et_2O was removed under vacuum and the residue was washed by *n*-hexane (5 mL). Then yellow solid was dissolved in THF (3 mL), and the solution was added to a solution of $[\{Cp^*IrCl_2\}_2]$ (197 mg, 0.25 mmol) in CH_3OH (15 mL). The mixture was stirred for 24 h after addition of pyridine (1 equiv). Finally, after evaporating the solvent under vacuum, a blue residue was isolated by column chromatography on silica gel with elution (CH_2Cl_2/CH_3OH, 15:1), thereby affording **6a** and **7a**.

For compound ***6a***: ^{1}H NMR (400 MHz, $CDCl_3$, 25 °C): $\delta = 1.48$ (s, 15H; Cp*), 7.45–7.95 ppm (m, 10H; phenyl); ^{11}B NMR (160 MHz, $CDCl_3$, 25 °C): $\delta = -2.98$ (1B), −7.56 (1B), −9.67 (1B), −15.61 (1B), −22.36 (2B), −26.99 (1B), −33.25 ppm (2B); ^{31}P NMR (162 MHz, $CDCl_3$, H_3PO_4, 25 °C): $\delta = 24.85$ ppm (s; $-P(S)Ph_2$); IR (KBr disk): $\tilde{\nu} = 2586$, 2554, 2521 (B–H), 1382 (C–H), 638 cm^{-1} (P=S); elemental analysis calcd (%) for $C_{24}H_{35}B_9IrPS_2$: C 40.70; H 4.98; found: C 40.65, H 5.03.

For compound ***7a***: ^{1}H NMR (400 MHz, $CDCl_3$, 25 °C): $\delta = 1.51$ (s, 15H; Cp*), 3.36 (s, 3H; OCH_3) 7.25–7.86 ppm (m, 10H; phenyl); ^{11}B NMR (160 MHz, $CDCl_3$, 25 °C): $\delta = 18.06$ (1B), −2.79 (1B), −7.81 (1B), −9.75 (1B), −11.65 (2B), −18.74 (1B), −21.97 (1B), −33.12 ppm (1B); ^{31}P NMR (162 MHz, $CDCl_3$, H_3PO_4, 25 °C): $\delta = 24.76$ ppm (s; $-P(S)Ph_2$); IR (KBr disk): $\tilde{\nu} = 2558$ (B–H), 1383 (C–H), 638 cm^{-1} (P=S); elemental analysis calcd (%) for $C_{25}H_{37}B_9IrOPS_2$: C 40.68, H 5.05; found: C 40.61, H 5.14.

Synthesis of 8a: A solution of nBuPPh_2 (24.2 mg, 0.1 mmol) in CH_3OH (5 mL) was added to a solution of **6a** (73.8 mg, 0.1 mmol) in CH_3OH (15 mL) at 0 °C. The solvent was removed under vacuum after stirring for 12 h, and the residue was washed twice with hexane (5 mL). Finally, **8a** was isolated by recrystallization from a CH_2Cl_2/Et_2O solution. Yield: 197.1 mg (77%) as a yellow powder. ^{1}H NMR (400 MHz, $CDCl_3$, 25 °C): $\delta = 0.81$ (m, 3H; $-CH_3$), 0.89 (m, 2H; $-CH_2$), 1.37 (d, $^4J(P,H) = 2.6$ Hz, 15H; Cp*), 1.67 (m, 2H; $-CH_2$), 1.93 (m, 2H; $-CH_2$), 7.44–7.93 ppm (m, 20H; phenyl); ^{11}B NMR (160 MHz, $CDCl_3$, 25 °C) $\delta = -1.57$ (1B), −8.54 (2B), −14.55 (2B), −17.98 (2B), −32.89 ppm (2B); ^{31}P NMR (162 MHz, $CDCl_3$, H_3PO_4, 25 °C): $\delta = 25.09$ (s; $-P(S)Ph_2$), −3.06 ppm (s; nBu$P$$Ph_2$); IR (KBr disk): $\tilde{\nu} = 2537$, 2523 (B–H), 1380 (C–H), 633 cm^{-1} (P=S); elemental analysis calcd (%) for $C_{40}H_{54}B_9IrP_2S_2$: C 50.55, H 5.72; found: C 50.54, H 5.69.

X-ray crystallography: Diffraction data of **1a**, **2a**, **3b**, **4b**, **5a**, **5b**, **7a**, and **8a** were collected using a Bruker Smart APEX CCD diffractometer with graphite-monochromated $Mo_{K\alpha}$ radiation ($\lambda = 0.71073$ Å). All the data were collected at room temperature and the structures were solved by direct methods and subsequently refined on F^2 by using full-matrix least-squares techniques (SHELXL).[20] SADABS[21] absorption corrections were applied to the data. All the non-hydrogen atoms were refined anisotropically, and hydrogen atoms were located at calculated positions. C_{cage}–H of **1a**, **3b**, **4b**, **5a**, and **5b**; H–B10, H–B11, and B10-H-B11 of **6a**; H–B9, H–B10, and H–B11 of **8a**; and H(1′)–Ir of **2a**) were found by the difference Fourier method. A summary of the crystallographic data and selected experimental information are given in Table 1.

CCDC-776662 (**1a**), 776663 (**2a**), 776664 (**3b**), 776665 (**4b**), 776666 (**5a**), 776667 (**5b**), 776669 (**7a**), and 776669 (**8a**) contain the supplementary crystallographic data for this paper. These data can be obtained free of charge from The Cambridge Crystallographic Data Centre via www.ccdc.cam.ac.uk/data_request/cif.

Acknowledgements

This work was supported by the National Science Foundation of China (20721063, 20771028), the Shanghai Science and Technology Committee (08DZ2270500, 08J1400103), the Shanghai Leading Academic Discipline Project (B108) and the National Basic Research Program of China (2009CB825300).

[1] a) M. F. Hawthorne, J. I. Zink, J. M. Skelton, M. J. Bayer, C. Liu, E. Livshits, R. Baer, D. Neuhauser, *Science* **2004**, *303*, 1849–1851; b) M. Juhasz, S. Hoffmann, E. Stoyanov, K. C. Kim, C. A. Reed, *Angew. Chem.* **2004**, *116*, 5466–5469; *Angew. Chem. Int. Ed.* **2004**, *43*, 5352–5355; c) R. N. Grimes, *J. Chem. Educ.* **2004**, *81*, 657–672; d) J. F. Valliant, K. J. Guenther, A. S. King, P. Morel, P. Schaffer, O. O. Sogbein, K. A. Stephenson, *Coord. Chem. Rev.* **2002**, *232*, 173–230; e) Y. Zhu, A. T. Peng, K. Carpenter, J. A. Maguire, N. S. Hosmane, M. Takagaki, *J. Am. Chem. Soc.* **2005**, *127*, 9875–9880; f) J. Q. Wang, M. Herberhold, G. X. Jin, *Organometallics* **2006**, *25*, 3508–3514; g) M. Herberhold, H. Yan, W. Milius, B. Wrackmeyer, *Chem. Eur. J.* **2000**, *6*, 3026–3032; h) X. Wang, G. X. Jin, *Chem. Eur. J.* **2005**, *11*, 5758–5764; i) Z. Qiu, Z. Xie, *Angew. Chem.* **2008**, *120*, 6674–6677; *Angew. Chem. Int. Ed.* **2008**, *47*, 6572–6575.

[2] a) D. Liu, L. Dang, Y. Sun, H. S. Chan, Z. Lin, Z. Xie, *J. Am. Chem. Soc.* **2008**, *130*, 16103–16110; b) G. L. Wang, Y. J. Lin, H. Berke, G. X. Jin, *Inorg. Chem.* **2008**, *47*, 2940–2942; c) H. Jude, H. Disteldorf, S. Fischer, T. Wedge, A. M. Hawkridge, A. M. Arif, M. F. Hawthorne, D. C. Muddiman, P. J. Stang, *J. Am. Chem. Soc.* **2005**, *127*, 12131–12139; d) S. Liu, Y F. Han, G. X. Jin, *Chem. Soc. Rev.* **2007**, *36*, 1543–1560; e) X. Meng, F. Wang, G. X. Jin, *Coord. Chem. Rev.* **2010**, *254*, 1260–1272; f) B. H. Xu, X. Q. Peng, Y. Z. Li, H. Yan, *Chem. Eur. J.* **2008**, *14*, 9347–9356.

[3] a) M. F. Hawthorne, A. Maderna, *Chem. Rev.* **1999**, *99*, 3421–3434; b) M. F. Hawthorne, Z. P. Zheng, *Acc. Chem. Res.* **1997**, *30*, 267–276; c) D. H. Wu, C. H. Wu, Y. Z. Li, D. D. Guo, X. M. Wang, H. Yan, *Dalton Trans.* **2009**, 285–290; d) C. H. Wu, D. H. Wu, X. Liu, G. Guoyiqibayi, D. D. Guo, G. Lv, X. M. Wang, H. Yan, H. Jiang, Z. H. Lu, *Inorg. Chem.* **2009**, *48*, 2352–2354.

[4] a) Z. Xie, *Acc. Chem. Res.* **2003**, *36*, 1–9; b) J. D. Lee, Y. J. Lee, K. C. Son, M. Cheong, J. Ko, S. O. Kang, *Organometallics* **2007**, *26*, 3374–3384; c) L. Deng, H. S. Chan, Z. Xie, *J. Am. Chem. Soc.* **2005**, *127*, 13774–13775; d) O. Tutusaus, C. Viñas, R. Núñez, F. Teixidor, A. Demonceau, S. Delfosse, A. F. Noels, I. Mata, E. Molins, *J. Am. Chem. Soc.* **2003**, *125*, 11830–11831; e) A. Felekidis, M. Goblet-Stachow, J. F. Liégeois, B. Pirotte, J. Delarge, A. Demonceau, M. Fontaine, A. F. Noel, I. T. Chizhevsky, T. V. Zinevich, V. I. Bregadze, F. M. Dolgushin, A. I. Yanovsky, Y. T. Struchkov, *J. Organomet. Chem.* **1997**, *536–537*, 405–412; f) B. Grüner, J. Plešek, J. Báča, I. Císařová, J. F. Dozol, H. Rouquette, C. Viñas, P. Selucký, J. Rais, *New J. Chem.* **2002**, *26*, 1519–1527; g) J. Plešek, B. Grüner, I. Císařová, J. Báča, P. Selucký, J. Rais, *J. Organomet. Chem.* **2002**, *657*, 59–70; h) J. Plešek, B. Grüner, S. Heřmánek, J. Báča, V. Mareček, J. Jänchenová, A. Lhotský, K. Holub, P. Selucký, J. Rais, I. Císařová, J. Cáslavský, *Polyhedron* **2002**, *21*, 975–986; i) A.-I. Stoica, C. Viñas, F. Teixidor, *Chem. Commun.* **2008**, 6492–6494.

[5] a) R. Núñez, C. Viñas, F. Teixidor, R. Sillanpää, R. Kivekäs, *J. Organomet. Chem.* **1999**, *592*, 22–28; b) C. Viñas, R. Núñez, F. Teixidor, R. Kivekäs, R. Sillanpää, *Organometallics* **1998**, *17*, 2376–2378; c) C. Viñas, R. Benakki, F. Teixidor, J. Casabó, *Inorg. Chem.* **1995**, *34*, 3844–3845.

[6] a) F. Teixidor, M. A. Flores, C. Viñas, R. Sillanpää, R. Kivekäs, *J. Am. Chem. Soc.* **2000**, *122*, 1963–1973; b) I. T. Chizhevsky, *Coord. Chem. Rev.* **2007**, *251*, 1590–1619; c) J. Llop, C. Viñas, F. Teixidor, L. Victori, R. Kivekäs, R. Sillanpää, *Organometallics* **2001**, *20*, 4024–4030; d) L. Alekseev, A. V. Safronov, F. M. Dolgushin, A. A. Korlyukov, I. A. Godovikov, I. T. Chizhevsky, *J. Organomet. Chem.* **2009**, *694*, 1727–1735; e) J. M. Oliva, N. L. Allan, P. von R. Schleyer, C. Viñas, F. Teixidor, *J. Am. Chem. Soc.* **2005**, *127*, 13538–13547.

[7] X. K. Huo, G. Su, G. X. Jin, *Dalton Trans.* **2010**, *39*, 1954–1961; a) F. Teixidor, A. Romeros, C. Viñas, J. Rius, C. Miravittles, J. Casabó, *J. Chem. Soc. Chem. Commun.* **1991**, 192–193; b) F. Teixidor, J. Casabó, A. M. Romerosa, C. Viñas, J. Rius, C. Miravittles, *J. Am. Chem. Soc.* **1991**, *113*, 9896–9898; c) J. I. van der Vlugt, *Angew. Chem.* **2010**, *122*, 260–263; *Angew. Chem. Int. Ed.* **2010**, *49*, 252–255.

[8] a) G. J. Kubas, *Chem. Rev.* **2007**, *107*, 4152–5205; b) B. Chin, A. J. Lough, R. H. Morris, C. T. Schweitzer, C. D′Agostino, *Inorg. Chem.* **1994**, *33*, 6278–6288; c) J. D. Gilbertson, N. K. Szymczak, D. R. Tyler, *Inorg. Chem.* **2004**, *43*, 3341–3343; d) N. K. Szymczak, L. N. Zakharov, D. R. Tyler, *J. Am. Chem. Soc.* **2006**, *128*, 15830–15835; e) J. D. Gilbertson, N. K. Szymczak, J. L. Crossland, W. K. Miller, D. K. Lyon, B. M. Foxman, J. Davis, D. R. Tyler, *Inorg. Chem.* **2007**, *46*, 1205–1214.

[9] a) Y. Ohki, M. Sakamoto, K. Tatsumi, *J. Am. Chem. Soc.* **2008**, *130*, 11610–11611; b) M. Vogt, V. Pons, D. M. Heinekey, *Organometallics* **2005**, *24*, 1832–1836; c) H. Kato, H. Seino, Y. Mizobe, M. Hidai, *Dalton Trans.* **2002**, 1494–1499.

[10] a) M. C. Brandys, R. J. Puddephatt, *J. Am. Chem. Soc.* **2002**, *124*, 3946–3950; b) P. Teo, L. L. Koh, T. S. A. Hor, *Inorg. Chem.* **2008**, *47*, 9561–9568; c) D. J. Eisler, R. J. Puddephatt, *Inorg. Chem.* **2005**, *44*, 4666–4678.

[11] a) Z. G. Zhang, T. S. A. Hor, *Polyhedron* **1995**, *14*, 2403–2409; b) B. D. Swartz, C. Nataro, *Organometallics* **2005**, *24*, 2447–2451; c) S. Büschel, C. Daniliuc, P. G. Jones, M. Tamm, *Organometallics* **2010**, *29*, 671–675.

[12] a) D. C. Apperley, N. Bricklebank, M. B. Hursthouse, M. E. Light, S. J. Coles, *Polyhedron* **2001**, *20*, 1907–1913; b) G. Pilloni, B. Longato, G. Bandoli, B. Corain, *J. Chem. Soc. Dalton Trans.* **1997**, 819–825.

[13] a) M. Gorol, H. W. Roesky, M. Noltemeyer, H. G. Schmidt, *Eur. J. Inorg. Chem.* **2005**, 4840–4844; b) F. Teixidor, C. Viñas, R. Sillanpää, R. Kivekäs, J. Casabó, *Inorg. Chem.* **1993**, *32*, 2645–2650; c) F. Teixidor, R. Benakki, C. Viñas, R. Kivekäs, R. Sillanpää, *Inorg. Chem.* **1999**, *38*, 5916–5919; d) F. Teixidor, R. Benakki, C. Viñas, R. Kivekäs, R. Sillanpää, *Organometallics* **1998**, *17*, 4630–4633.

[14] K. Hesp, R. McDonald, M. Ferguson, M. Stradiotto, *J. Am. Chem. Soc.* **2008**, *130*, 16394–16406.

[15] J. Y. Bae, Y. I. Park, J. Ko, K. I. Park, S. I. Cho, S. O. Kang, *Inorg. Chim. Acta* **1999**, *289*, 141–148.

[16] D. Sellmann, M. Geck, F. Knoch, G. Ritter, J. Dengler, *J. Am. Chem. Soc.* **1991**, *113*, 3819–3828.

[17] a) J. Q. Wang, S. Cai, G. X. Jin, L. H. Weng, M. Herberhold, *Chem. Eur. J.* **2005**, *11*, 7342–7350; b) S. Cai, J. Q. Wang, G. X. Jin, *Organometallics* **2005**, *24*, 4226–4231; c) G. X. Jin, J. Q. Wang, C. Zhang, L. H. Weng, M. Herberhold, *Angew. Chem.* **2005**, *117*, 264–267; *Angew. Chem. Int. Ed.* **2005**, *44*, 259–262; d) S. Cai, Y. J. Lin, G. X. Jin, *Dalton Trans.* **2006**, 912–918.

[18] W. D. Jones, V. L. Kuykendall, *Inorg. Chem.* **1991**, *30*, 2615–2622.

[19] C. White, A. Yates, P. M. Maitlis, *Inorg. Synth.* **1992**, *29*, 228–234.

[20] SHELXL-97 Program for the Refinement of Crystal Structures, G. M. Sheldrick, Universität Göttingen (Germany), **1997**.

[21] SADABS 2.01, Bruker/Siemens Area Detector Absorption Correction Program, G. M. Sheldrick, Bruker AXS, Madison, WI, **1998**.

Received: May 12, 2010
Published online: September 8, 2010

